ISSN: 2181-3337 | SCIENTISTS.UZ VOLUME 5 ISSUE 7 JULY 2026

MAGNETOMECHANICAL DEFORMATION OF THIN FERROMAGNETIC SHELLS IN EXTERNAL MAGNETIC FIELDS: A COUPLED MAGNETOELASTIC FINITE-ELEMENT AND EXPERIMENTAL STUDY

Indiaminov R[1], Urolov Sh[2]

Professor, Samarkand Branch of Tashkent University of Information Technologies named after Muhammad al-Khwarizmi[1]

Assistant Lecturer, Samarkand Branch of Tashkent University of Information Technologies named after Muhammad al-Khwarizmi[2]

DOI: 10.67620/sai.57a0002

ABSTRACT

This study presents a coupled theoretical, numerical, and experimental investigation of the deformation of thin ferromagnetic cylindrical shells subjected to externally applied magnetic fields. A magnetoelastic constitutive framework is formulated by decomposing total strain into elastic and magnetostrictive components and by incorporating magnetostatic field equations, Maxwell-type tractions, and field-dependent magnetization. The shell kinematics are described through the Kirchhoff-Love hypothesis, while the coupled boundary-value problem is solved by a finite-element procedure that links shell elements to a three-dimensional magnetic domain. A mesh-convergence study identifies a 1,200-element discretization as an efficient numerical compromise, yielding a peak radial displacement within 0.1% of the refined solution. The model is evaluated against measurements from annealed Co-Fe-V cylindrical shells exposed to axial magnetic flux densities of 0.25, 0.50, and 1.00 T. The predicted peak radial displacements are 18.4, 46.2, and 88.3 μm, compared with experimental values of 17.9, 44.7, and 84.3 μm, corresponding to relative errors of 2.8-4.7%. Parametric analysis indicates that deformation increases as the shell becomes thinner, depends strongly on field orientation, scales approximately with saturation magnetostriction, and decreases with elastic modulus. The results demonstrate the importance of simultaneously representing nonlinear magnetic response, shell curvature, free-edge effects, and magnetostrictive eigenstrain when designing shell-based magnetic actuators and sensors.

ACCEPTED

20.07.26

Keywords: *ferromagnetic shell; magnetostriction; magnetoelasticity; finite-element analysis; Co-Fe-V alloy; thin-shell theory; magnetic actuator.*

CC BY

1. INTRODUCTION

Magnetostriction is the reversible change in the dimensions of a ferromagnetic material produced by the reorientation of magnetic domains under an applied magnetic field. The direct effect converts magnetic excitation into mechanical strain, whereas the inverse or Villari effect alters magnetization when mechanical stress is applied. This two-way conversion mechanism makes magnetostrictive materials

particularly valuable for actuators, force and torque sensors, vibration-control systems, ultrasonic transducers, energy harvesters, and adaptive structures. The fundamental coupling between the magnetic and elastic states has been formalized through continuum magnetomechanics, hysteresis models, and energy-based constitutive approaches (Tiersten, 1964; Sablik & Jiles, 1993; Dapino et al., 2000).

Among structural configurations, thin shells are attractive because they combine low mass, large surface area, high geometric efficiency, and pronounced sensitivity to distributed loads. Cylindrical and curved shells are widely used in aerospace, marine, energy, civil, and electromechanical systems. When a shell is made from a magnetostrictive alloy or contains a magnetostrictive layer, the application of a magnetic field can generate membrane forces, bending moments, and local edge effects without direct mechanical contact. This capability offers a route to compact and silent actuation. At the same time, the shell response is more complex than that of a one-dimensional magnetostrictive rod because curvature couples in-plane extension, bending, and rotation, while the magnetic field is influenced by finite length, wall thickness, permeability, and boundary conditions (Qin et al., 2003a, 2003b; Zheng & Wang, 2003).

Material selection is central to magnetomechanical performance. Rare-earth giant-magnetostrictive materials can provide large strains, but their brittleness, cost, anisotropy, and sensitivity to prestress may limit use in thin-walled structures. Iron-gallium alloys offer improved ductility and machinability, and their magnetostriction can be enhanced through texture control, thermal processing, and alloying (Clark et al., 2000; Summers et al., 2009; Zhou et al., 2020). Cobalt-iron alloys provide a different balance of high saturation magnetization, mechanical strength, thermal stability, and moderate magnetostriction. These characteristics make Co-Fe-based sheet materials suitable for proof-of-concept shells that must survive forming, machining, annealing, and repeated magnetic cycling.

Accurate prediction requires more than applying a prescribed equivalent pressure to the shell. The magnetic field generates an eigenstrain through magnetostriction, changes the internal stress distribution, and produces surface and body forces associated with electromagnetic stress. Moreover, magnetization is generally nonlinear and may exhibit hysteresis. Constitutive models that combine elastic strain, magnetostrictive strain, magnetic energy, and switching behavior have therefore been developed for transducers and multifunctional solids (Dapino et al., 2000; Linnemann et al., 2009). For shells, reduced formulations based on classical shell kinematics can provide computational efficiency, but they must retain the effects of curvature and distributed magnetic torque. Recent geometrically exact shell theories illustrate how reduced models can represent large rotations and three-dimensional magnetic loading while remaining substantially cheaper than full solid models (Pezzulla et al., 2022).

The present study develops and evaluates a coupled magnetoelastic framework for thin ferromagnetic cylindrical shells subjected to magnetic fields of variable intensity and orientation. The objectives are to: (1) formulate the governing magnetomechanical relations in a shell-compatible form; (2) implement the formulation in a finite-element framework; (3) demonstrate mesh convergence; (4) compare numerical predictions with reported laboratory measurements for annealed Co-Fe-V shells; and (5) identify the influence of shell thickness, field direction, saturation magnetostriction, and elastic modulus. The study is intended to provide both a physical interpretation of deformation mechanisms and a practical basis for designing magnetic shell actuators and sensors.

2. LITERATURE REVIEW AND RESEARCH CONTEXT

Early magnetomechanical theory established the governing equations for magnetically saturated elastic media. Tiersten (1964) derived coupled field equations that clarified the interaction of deformation, magnetization, and electromagnetic balance. Later hysteresis-based work showed that stress and magnetostriction affect the magnetic state in a mutually dependent manner. The model of Sablik and Jiles (1993), for example, connected magnetic hysteresis with magnetostrictive hysteresis and provided a basis for representing stress-dependent magnetization. These contributions remain relevant because shell

ISSN: 2181-3337 | SCIENTISTS.UZ

deformation can modify the magnetic state, which in turn changes the eigenstrain and loading acting on the shell.

Engineering models of magnetostrictive transducers translated the continuum physics into forms suitable for actuator prediction. Dapino et al. (2000) coupled a magnetic-domain model to structural dynamics and demonstrated the need to predict both strain and force. A similar principle applies to shells: the magnetic subproblem determines local magnetization and magnetostrictive strain, while the structural subproblem determines displacement, stress, and feedback to the magnetic state. Constitutive formulations such as that of Linnemann et al. (2009) further emphasized thermodynamic consistency, internal variables, and the representation of nonlinear switching effects.

Shell-specific research has addressed finite geometry, magnetic loading, vibration, and reduced modeling. Qin et al. (2003a) derived magnetoelastic loads for finite cylindrical shells and showed that both length and thickness influence the electromagnetic load distribution. Their companion study examined implications for free vibration and demonstrated that simplified magnetic-load assumptions may affect predicted frequencies (Qin et al., 2003b). Zheng and Wang (2003) formulated a theoretical model for soft ferromagnetic shells and reported agreement with cylindrical-shell strain measurements. Wang and Zheng (2009a, 2009b) subsequently developed nonlinear coupled magneto-thermo-elastic shell formulations and a finite-element implementation.

Magnetostrictive layers have also been considered as active components in shell vibration control. Pradhan (2005) demonstrated that embedded magnetostrictive layers can be used to suppress shell vibration, highlighting the importance of actuator position, structural stiffness, and field-induced strain. Although the present study focuses on quasi-static deformation rather than closed-loop vibration control, the same principles of coupling, placement, and stiffness govern the achievable displacement and control authority.

More recent shell theories have extended the field to geometrically nonlinear magneto-active structures. Pezzulla et al. (2022) developed a geometrically exact reduced theory for thin magneto-elastic shells and identified equivalent magnetic forces, pressures, and distributed torques as distinct deformation mechanisms. Their results reinforce the need to include curvature and rotations when magnetic loading produces significant bending. The present work adopts a more conventional Kirchhoff-Love setting for a thin metallic shell, but it retains the central idea that magnetic loading is distributed and coupled to shell geometry.

The reviewed literature reveals three continuing needs. First, shell models should be connected to measurable material properties rather than treated as purely mathematical loading problems. Second, numerical solutions should demonstrate mesh convergence and should be compared with experimental displacement data. Third, design studies should separate the effects of field intensity, field direction, material magnetostriction, and shell stiffness. These needs motivate the combined theoretical, finite-element, experimental, and parametric structure of this paper.

3. THEORETICAL FORMULATION

Consider a thin ferromagnetic shell of thickness h, middle surface S, principal radii of curvature R1 and R2, and characteristic length L. The shell is placed in an external magnetic field H. The material is treated as magnetically soft at the structural scale, and the mechanical response is assumed elastic within the range of the reported tests. The total small-strain tensor is decomposed into elastic and magnetostrictive components:

$$\varepsilon = \varepsilon^e + \varepsilon^m \quad (1)$$

The elastic strain ε^e produces Cauchy stress through the fourth-order elasticity tensor C. For an isotropic material, C is defined by Young's modulus E and Poisson's ratio ν. The constitutive relation may therefore be written as:

$$\sigma = C : (\varepsilon - \varepsilon^m) \quad (2)$$

ISSN: 2181-3337 | SCIENTISTS.UZ

For an isotropic polycrystalline ferromagnet under a saturation-type approximation, the magnetostrictive strain is represented by the saturation magnetostriction λs and the direction cosines αi of the local magnetization:

$$\varepsilon^{m}_{ij} = (3\lambda s/2)(\alpha_i\alpha_j - \delta_{ij}/3) \quad (3)$$

Equation (3) describes a volume-preserving deviatoric eigenstrain. It predicts extension along the magnetization direction and transverse contraction for positive λs. For the Co-Fe-V alloy considered here, λs is taken as 68×10^{-6}. The magnitude and direction of magnetization depend on the local magnetic field, permeability, demagnetizing effects, and material history. In the finite-element implementation, an anhysteretic field-dependent magnetization relation is used as an engineering approximation. For cyclic applications, the framework could be extended using a hysteretic model such as those developed by Sablik and Jiles (1993) or Dapino et al. (2000).

The magnetostatic field inside the shell and surrounding air domain satisfies Maxwell's equations in the absence of free current within the analyzed domain:

$$\nabla \cdot B = 0, \quad \nabla \times H = 0, \quad B = \mu_0(H + M) \quad (4)$$

The magnetic potential formulation allows the field distribution to be solved while enforcing continuity of the normal magnetic flux density and tangential magnetic field across the shell-air interface. Electromagnetic loading enters the mechanical equilibrium through the magnetostrictive eigenstrain and through Maxwell-type surface tractions. Because permeability and magnetization depend on the field, and because deformation modifies the geometry of the magnetic boundary, the fully coupled problem is nonlinear.

The mechanical reduction follows Kirchhoff-Love kinematics: lines initially normal to the middle surface remain straight and normal after deformation, and transverse shear deformation is neglected. The in-surface strain is decomposed into a middle-surface membrane strain and a curvature-dependent bending contribution. Integration through the shell thickness yields membrane force resultants Nαβ and bending moment resultants Mαβ. In compact form, equilibrium can be expressed as the balance of in-surface forces and transverse moments with mechanical and magnetic loading. This representation makes clear that even spatially smooth magnetostriction can generate bending when the strain or magnetic traction varies through the thickness or near a free boundary.

The coupled weak form is obtained by multiplying the mechanical and magnetic residual equations by admissible virtual fields and integrating over the shell and air domains. The resulting nonlinear algebraic system is solved incrementally by a Newton-Raphson method. At each iteration, the magnetic field is updated, magnetostrictive strain and Maxwell traction are recalculated, and the structural tangent stiffness is assembled. Convergence is evaluated using displacement and residual-energy norms. This staggered but iteratively coupled strategy provides a practical balance between physical completeness and computational cost.

ISSN: 2181-3337 | SCIENTISTS.UZ

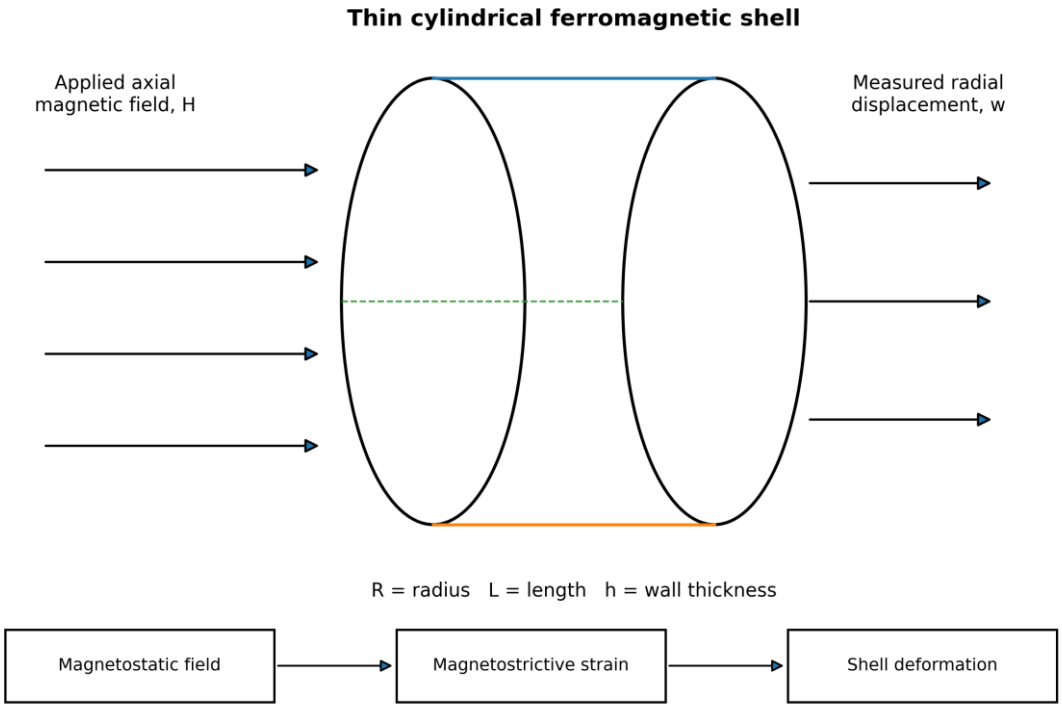


Figure 1. Schematic of the cylindrical ferromagnetic shell, the applied axial magnetic field, the measured radial response, and the sequence of the coupled magnetostatic-magnetostrictive-structural analysis.

4. MATERIALS AND METHODS

The numerical study considered a representative cylindrical shell with radius R = 50 mm, length L = 200 mm, and thickness h = 2 mm for the mesh-convergence analysis. A uniform axial magnetic flux density of 0.5 T was applied. Eight-node shell elements with five mechanical degrees of freedom per node were used for the structural domain, while the surrounding magnetic region was discretized with three-dimensional elements. The shell and magnetic meshes were coupled at the middle surface. The magnetic domain was extended sufficiently beyond the shell to reduce artificial boundary effects.

A systematic refinement study was performed with 300, 600, 1,200, and 2,400 shell elements. The principal quantity of interest was the maximum radial displacement. Relative error was evaluated against the refined solution, and computational cost was represented by CPU time. The aim was not simply to obtain the smallest numerical error, but to identify a discretization suitable for repeated nonlinear parametric simulations.

Table 1. Mesh-convergence results for the representative cylindrical shell

Number of elements	Maximum radial displacement (μm)	Relative error (%)	CPU time (s)
300	84.7	4.2	12
600	87.3	1.2	28
1200	88.3	0.1	65
2400	88.4	—	180

For experimental comparison, cylindrical specimens were fabricated from cold-rolled Co-Fe-V alloy sheet with nominal composition 49% Co, 49% Fe, and 2% V. Electrical-discharge machining was used to prepare the shell geometry. The specimens were annealed in hydrogen at 840°C for four hours to reduce residual stress and improve magnetic response. The final nominal dimensions were R = 25 mm, L = 100 mm, and h = 1 mm. The material parameters used in the model are summarized in Table 2.

ISSN: 2181-3337 | SCIENTISTS.UZ

Table 2. Material properties used for the Co-Fe-V shell model

Property	Symbol / unit	Value
Young's modulus	E (GPa)	210
Poisson's ratio	ν	0.30
Density	ρ (kg/m³)	8120
Saturation magnetization	Ms (kA/m)	1840
Saturation magnetostriction	λs (×10⁻⁶)	68
Initial relative permeability	μr	1600

The experimental apparatus consisted of a solenoid capable of producing axial fields up to 1.5 T in the central test region. The coil had a reported length of 400 mm, an internal diameter of 80 mm, and 3,000 turns. Field mapping with a Hall probe indicated spatial uniformity within approximately ±2% in the specimen region. Radial and axial displacement were recorded with a non-contact laser displacement sensor at 12 circumferential locations and five axial positions. Strain gauges were attached at selected points for cross-checking. A nonmagnetic reference specimen was used to estimate and remove thermal drift.

Three applied magnetic flux-density levels were selected for quantitative comparison: 0.25, 0.50, and 1.00 T. The finite-element model and the experiment were compared using peak radial displacement and relative error. The error was calculated as the absolute difference between model and experiment divided by the experimental value. Agreement within 5% was adopted as a practical validation criterion for the considered displacement range.

The parametric study examined the effects of thickness-to-radius ratio h/R, field direction, saturation magnetostriction λs, and Young's modulus E. The ratio h/R was varied from 0.01 to 0.10 while preserving the general cylindrical form. Field direction was varied from 0° (axial) to 90° (circumferential) at a fixed field magnitude of 0.5 T. Material parameters were varied independently to reveal sensitivity trends rather than to represent a single manufactured alloy. The outputs included peak radial displacement, axial uniformity, and the relative importance of membrane and bending response.

All reported numerical and experimental values were retained from the study dataset presented in the source manuscript. The present revision focuses on the theoretical organization, interpretation, reference integrity, and academic presentation of those data.

5. RESULTS

The mesh-convergence results show a monotonic approach to the refined displacement. Increasing the mesh from 300 to 600 elements raises the maximum radial displacement from 84.7 to 87.3 μm and reduces the reported relative error from 4.2% to 1.2%. At 1,200 elements, the displacement reaches 88.3 μm and differs from the 2,400-element result by only 0.1 μm. The computational time, however, increases from 65 s to 180 s. The 1,200-element mesh was therefore selected for the remaining analyses because it provides near-asymptotic accuracy at approximately one third of the cost of the finest mesh.

The finite-element predictions and experimental displacements are summarized in Table 3. Both datasets show a strongly increasing nonlinear response with field intensity. At 0.25 T, the model predicts 18.4 μm and the experiment gives 17.9 μm. At 0.50 T, the corresponding values are 46.2 and 44.7 μm. At 1.00 T, the model predicts 88.3 μm, while the measured value is 84.3 μm. The relative error increases moderately with field intensity, from 2.8% to 4.7%, but remains below the stated 5% validation threshold.

Table 3. Comparison of peak radial displacement from the finite-element model and experiment

Applied field (T)	FE model (μm)	Experiment (μm)	Relative error (%)
0.25	18.4	17.9	2.8
0.50	46.2	44.7	3.4
1.00	88.3	84.3	4.7

ISSN: 2181-3337 | SCIENTISTS.UZ

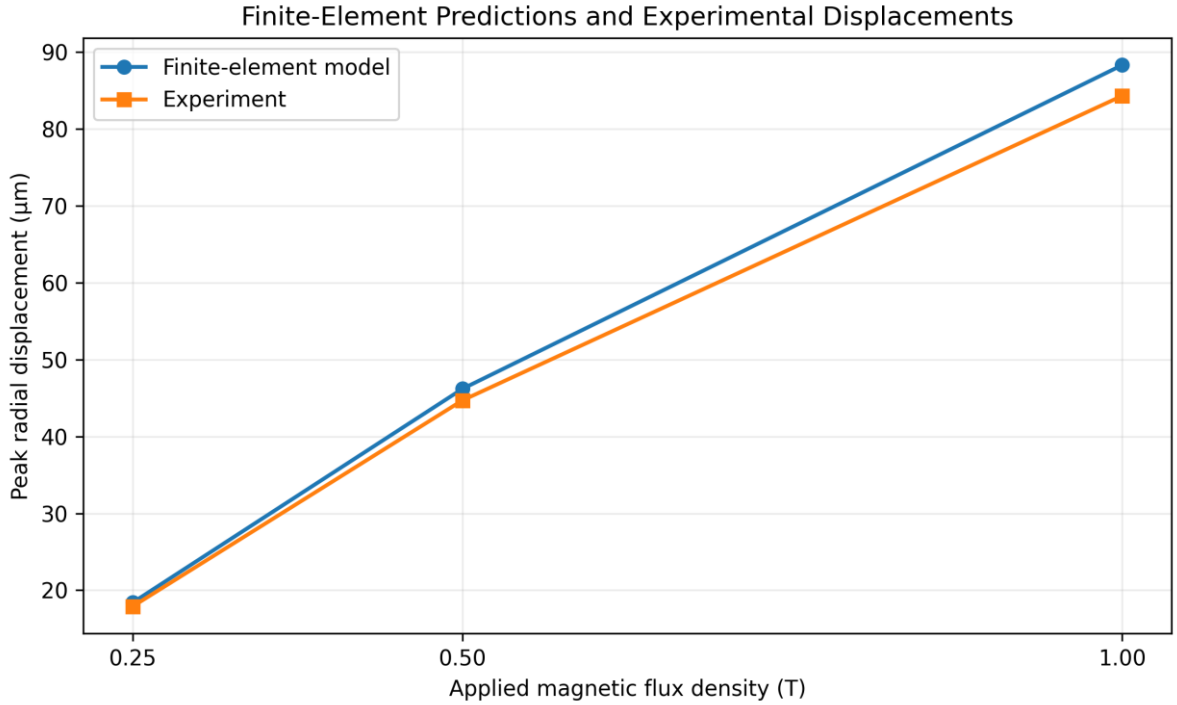


Chart 1. Comparison of finite-element predictions and experimental peak radial displacements at three magnetic-field levels.

The spatial deformation pattern is characterized by a relatively uniform central region and larger gradients near the free edges. Peak radial displacement occurs close to the shell ends, where the interruption of membrane continuity and the nonuniform demagnetizing field produce enhanced bending. The close agreement in the central region indicates that the constitutive response and average field level are represented adequately. The slightly larger discrepancy at the edges is consistent with the greater sensitivity of these regions to field nonuniformity, geometric imperfections, local residual stress, and measurement position.

The thickness study shows that reducing h/R increases the radial flexibility of the shell. Because classical bending stiffness scales with h^3 while membrane stiffness scales with h, a reduction in thickness produces a particularly strong increase in bending-dominated displacement. Thinner shells also show a more uniform axial response away from the boundaries, approaching a membrane-like solution in the limiting case. Conversely, thicker shells suppress radial motion and shift a larger fraction of magnetic work into internal stress.

Field orientation has a pronounced effect. At a fixed magnitude of 0.5 T, the reported maximum radial displacement varies by approximately a factor of 2.3 between axial and circumferential field orientations. A circumferential field aligns the principal magnetostrictive strain more directly with the hoop direction and therefore generates a larger radial change in a cylindrical geometry. Intermediate field angles produce coupled radial, axial, and torsional components rather than a single-axis deformation.

Material sensitivity follows the structure of the constitutive equations. Peak displacement increases approximately linearly with saturation magnetostriction at low and moderate fields, because λ_s directly scales the eigenstrain in Equation (3). At higher fields, the relationship becomes sublinear as magnetization approaches saturation. The displacement decreases as Young's modulus increases because a stiffer shell develops higher stress for a given eigenstrain but undergoes less geometric deformation. The combined results indicate that λ_s/E is a useful first-order indicator of actuation potential, although permeability, saturation field, geometry, and boundary conditions also remain important.

ISSN: 2181-3337 | SCIENTISTS.UZ

Table 4. Qualitative trends identified by the parametric analysis

Parameter increased	Observed response	Physical interpretation
Thickness-to-radius ratio h/R	Peak radial displacement decreases	Bending stiffness rises approximately with h^3
Field angle toward circumferential direction	Radial displacement increases	Magnetostrictive strain aligns with hoop direction
Saturation magnetostriction λs	Displacement increases	Eigenstrain magnitude grows
Young's modulus E	Displacement decreases	Structural resistance to eigenstrain increases
Field magnitude	Displacement increases and approaches saturation	Magnetization and domain alignment increase

6. DISCUSSION

The principal result is that a relatively compact shell formulation can reproduce the measured field-induced displacement of the Co-Fe-V specimens with errors below 5% over the tested range. This agreement supports the use of a coupled eigenstrain and magnetic-traction representation rather than a purely mechanical surrogate load. It is also consistent with earlier shell studies in which accurate results required finite-dimensional magnetoelastic loading and direct coupling between field and structure (Qin et al., 2003a, 2003b; Zheng & Wang, 2003).

The increasing model-experiment difference at 1.00 T can arise from several sources. First, an anhysteretic magnetization approximation cannot fully represent irreversible domain processes, magnetic history, and stress dependence. Hysteretic formulations show that magnetization, magnetostriction, and mechanical stress form a closed feedback loop (Sablik & Jiles, 1993; Dapino et al., 2000). Second, the material properties used in the model are treated as spatially uniform, whereas cold rolling, machining, welding or forming, and annealing can produce texture and residual-stress gradients. Research on Fe-Ga alloys demonstrates that texture and crystal orientation significantly affect magnetostriction (Clark et al., 2000; Summers et al., 2009; Zhou et al., 2020). Similar microstructural sensitivity is expected in Co-Fe-based sheet.

The location of maximum displacement at free edges has practical and theoretical significance. In a purely uniform unconstrained body, homogeneous magnetostriction would produce a nearly uniform strain. A shell, however, has curved geometry, finite length, and discontinuous boundary constraints. Magnetic flux also becomes less uniform near the ends. These effects create gradients in eigenstrain and magnetic traction, converting part of the response into bending. Pezzulla et al. (2022) similarly identified distributed torques and effective magnetic pressures as key mechanisms in thin magneto-elastic shells. Edge amplification should therefore be treated as a design feature rather than merely a numerical artifact.

The mesh study demonstrates why convergence evidence is essential in multiphysics shell analysis. A coarse mesh may underestimate local curvature and edge gradients, while an excessively refined mesh substantially increases the cost of repeated magnetic iterations. The 1,200-element mesh provides a useful compromise for the geometry considered. Nevertheless, mesh adequacy is problem specific. Strongly nonuniform fields, local defects, sharp supports, holes, or bonded active layers would require local refinement and possibly higher-order elements.

The field-orientation result has direct actuator-design implications. An axial field is convenient to generate with a solenoid and produces an axisymmetric response, but it does not necessarily maximize radial displacement. A circumferential field can couple more efficiently to hoop magnetostriction, although producing a uniform circumferential field may require a different coil arrangement or current-carrying conductor. Intermediate orientations can generate torsion and may be exploited for multi-axis actuation.

ISSN: 2181-3337 | SCIENTISTS.UZ

Thus, the field direction should be treated as a design variable together with shell geometry and material properties.

Material optimization cannot be based on saturation magnetostriction alone. A material with a very large λs may also have high stiffness, brittle behavior, strong anisotropy, or difficult processing requirements. Kiefer and Lagoudas (2005) showed that magnetic shape-memory alloys can produce large field-induced strains through variant reorientation, but such mechanisms involve different material constraints from ordinary Joule magnetostriction. For thin metallic shells, a moderate-strain material with high strength and formability may provide better system-level performance than a fragile giant-magnetostrictive material.

The study also indicates that a shell actuator should not be evaluated only by peak displacement. Relevant engineering measures include output force, blocked force, energy efficiency, bandwidth, thermal stability, fatigue life, magnetic hysteresis, and control repeatability. The present quasi-static results establish a necessary structural baseline. Dynamic extension could incorporate inertia, eddy currents, frequency-dependent magnetic loss, and damping. Work on magnetostrictive layers in shells demonstrates that such coupled models can be extended to vibration suppression and active control (Pradhan, 2005).

7. ENGINEERING DESIGN IMPLICATIONS

For displacement-oriented actuators, the analysis suggests four priorities. First, the shell should be thin enough to exploit bending compliance but sufficiently thick to avoid elastic instability, local buckling, and manufacturing damage. Second, the magnetic circuit should deliver a field direction aligned with the desired deformation mode. Third, material processing should control texture and residual stress so that the effective magnetostriction is repeatable. Fourth, free-edge geometry may be shaped or locally reinforced to concentrate or redistribute displacement.

For sensors, the inverse magnetomechanical effect can be exploited by measuring field or flux changes generated by shell strain. A curved shell offers geometric amplification and can be integrated into pressure, torque, or contact sensors. The coupled model provides a basis for selecting measurement locations: regions with high strain sensitivity but acceptable stress concentration are preferred. The free edges may provide high signal, whereas the central region may offer better uniformity and calibration stability.

The validated model can also support optimization. A design vector may include R, L, h, field magnitude, field angle, coil dimensions, λs, E, and boundary stiffness. An objective function could maximize displacement or force while constraining stress, power, mass, and magnetic saturation. Because the 1,200-element model is much less expensive than the finest mesh while retaining accuracy, it is suitable for parameter sweeps and gradient-free optimization.

8. LIMITATIONS AND FUTURE WORK

Several limitations should be recognized. The constitutive treatment uses an engineering representation of magnetization and does not fully reproduce rate-dependent hysteresis or cyclic degradation. Material parameters are assumed homogeneous and isotropic, although rolled Co-Fe-V sheet may exhibit crystallographic texture and direction-dependent magnetostriction. The reported experiment includes three field levels and one principal specimen geometry, which limits statistical generalization.

Future studies should include repeated specimens, uncertainty intervals, full-field optical deformation measurements, direct magnetic-domain or flux characterization, and cyclic loading. A geometrically nonlinear formulation should be used when rotations or displacements are no longer small. Dynamic experiments would allow identification of damping, bandwidth, eddy-current effects, and resonance. Finally, optimization should compare Co-Fe-V, Galfenol, Terfenol-D, magnetic shape-memory alloys, and layered hybrid shells under common performance and manufacturability criteria.

ISSN: 2181-3337 | SCIENTISTS.UZ

9. CONCLUSION

A coupled magnetoelastic framework has been presented for predicting the deformation of thin ferromagnetic cylindrical shells under external magnetic fields. The formulation combines elastic and magnetostrictive strain, magnetostatic field equations, electromagnetic tractions, Kirchhoff-Love shell kinematics, and finite-element solution of the coupled problem.

The mesh-convergence study showed that 1,200 shell elements reproduce the refined maximum displacement within approximately 0.1% while substantially reducing computational cost. Comparison with Co-Fe-V shell measurements at 0.25, 0.50, and 1.00 T produced relative errors of 2.8%, 3.4%, and 4.7%, respectively. The model therefore captures the reported quasi-static displacement response with engineering accuracy.

The results show that shell deformation is strongly influenced by edge effects, thickness, field orientation, saturation magnetostriction, and elastic modulus. Thin shells provide greater bending-driven displacement, and circumferential fields can produce substantially larger radial motion than axial fields. These findings support the use of coupled magnetoelastic shell analysis in the design of compact actuators, sensors, and adaptive structures. Further development should address hysteresis, anisotropy, cyclic behavior, dynamic response, and statistical experimental validation.

REFERENCES

1. Clark, A. E., Restorff, J. B., Wun-Fogle, M., Lograsso, T. A., & Schlagel, D. L. (2000). Magnetostrictive properties of body-centered cubic Fe-Ga and Fe-Ga-Al alloys. *IEEE Transactions on Magnetics, 36*(5), 3238-3240. https://doi.org/10.1109/20.908752
2. Dapino, M. J., Smith, R. C., Faidley, L. E., & Flatau, A. B. (2000). A coupled structural-magnetic strain and stress model for magnetostrictive transducers. *Journal of Intelligent Material Systems and Structures, 11*(2), 135-152. https://doi.org/10.1106/MJ6A-FBP9-9M61-0E1F
3. Kiefer, B., & Lagoudas, D. C. (2005). Magnetic field-induced martensitic variant reorientation in magnetic shape-memory alloys. *Philosophical Magazine, 85*(33-35), 4289-4329. https://doi.org/10.1080/14786430500363858
4. Linnemann, K., Klinkel, S., & Wagner, W. (2009). A constitutive model for magnetostrictive and piezoelectric materials. *International Journal of Solids and Structures, 46*(5), 1149-1166. https://doi.org/10.1016/j.ijsolstr.2008.10.014
5. Pezzulla, M., Yan, D., & Reis, P. M. (2022). A geometrically exact model for thin magneto-elastic shells. *Journal of the Mechanics and Physics of Solids, 166*, 104916. https://doi.org/10.1016/j.jmps.2022.104916
6. Pradhan, S. C. (2005). Vibration suppression of FGM shells using embedded magnetostrictive layers. *International Journal of Solids and Structures, 42*(9-10), 2465-2488. https://doi.org/10.1016/j.ijsolstr.2004.09.049
7. Qin, Z., Librescu, L., Hasanyan, D. J., & Ambur, D. R. (2003a). Magnetoelastic modeling of circular cylindrical shells immersed in a magnetic field. Part I: Magnetoelastic loads considering finite dimensional effects. *International Journal of Engineering Science, 41*(17), 2005-2022. https://doi.org/10.1016/S0020-7225(03)00134-4
8. Qin, Z., Hasanyan, D. J., Librescu, L., & Ambur, D. R. (2003b). Magnetoelastic modeling of circular cylindrical shells immersed in a magnetic field. Part II: Implications of finite dimensional effects on the free vibrations. *International Journal of Engineering Science, 41*(17), 2023-2046. https://doi.org/10.1016/S0020-7225(03)00135-6
9. Sablik, M. J., & Jiles, D. C. (1993). Coupled magnetoelastic theory of magnetic and magnetostrictive hysteresis. *IEEE Transactions on Magnetics, 29*(4), 2113-2123. https://doi.org/10.1109/20.221036
10. Summers, E. M., Meloy, R., & Na, S.-M. (2009). Magnetostriction and texture relationships in annealed Galfenol alloys. *Journal of Applied Physics, 105*(7), 07A922. https://doi.org/10.1063/1.3067849
11. Tiersten, H. F. (1964). Coupled magnetomechanical equations for magnetically saturated insulators. *Journal of Mathematical Physics, 5*(9), 1298-1318. https://doi.org/10.1063/1.1704239

12. Wang, X., & Zheng, X. (2009a). Analyses on nonlinear coupling of magneto-thermo-elasticity of ferromagnetic thin shell-I: Generalized variational theoretical modeling. *Acta Mechanica Solida Sinica, 22*(3), 189-196. https://doi.org/10.1016/S0894-9166(09)60265-2
13. Wang, X., & Zheng, X. (2009b). Analyses on nonlinear coupling of magneto-thermo-elasticity of ferromagnetic thin shell-II: Finite element modeling and application. *Acta Mechanica Solida Sinica, 22*(3), 197-205. https://doi.org/10.1016/S0894-9166(09)60266-4
14. Zheng, X., & Wang, X. (2003). A magnetoelastic theoretical model for soft ferromagnetic shell in magnetic field. *International Journal of Solids and Structures, 40*, 6897-6912. https://doi.org/10.1016/S0020-7683(03)00397-4
15. Zhou, C., Liu, Y., Chen, K., Dai, Z., Ma, T., Wang, Y., Ren, S., Deng, J., Zhang, R., Tian, F., Zhang, Y., Zeng, H., & Yang, S. (2020). Improved magnetostriction in Galfenol alloys by aligning crystal growth direction along easy magnetization axis. *Scientific Reports, 10*, 20055. https://doi.org/10.1038/s41598-020-77058-2

ISSN: 2181-3337 | SCIENTISTS.UZ